Oxytocin under opioid antagonism leads to supralinear enhancement of social attention

Olga Dal Monte[a,1,2], Matthew Piva[a,b,c,1], Kevin M. Anderson[a], Marios Tringides[a], Avram J. Holmes[a,c,d,e], and Steve W. C. Chang[a,b,c]

[a]Department of Psychology, Yale University, New Haven, CT 06520; [b]Department of Neuroscience, Yale University School of Medicine, New Haven, CT 06510; [c]Interdepartmental Neuroscience Program, Yale University School of Medicine, New Haven, CT 06510; [d]Department of Psychiatry, Yale University School of Medicine, New Haven, CT 06510; and [e]Department of Psychiatry, Massachusetts General Hospital, Boston, MA 02114

Edited by Katalin M. Gothard, The University of Arizona, Tucson, and accepted by Editorial Board Member Marlene Behrmann April 3, 2017 (received for review February 16, 2017)

To provide new preclinical evidence toward improving the efficacy of oxytocin (OT) in treating social dysfunction, we tested the benefit of administering OT under simultaneously induced opioid antagonism during dyadic gaze interactions in monkeys. OT coadministered with a μ-opioid receptor antagonist, naloxone, invoked a supralinear enhancement of prolonged and selective social attention, producing a stronger effect than the summed effects of each administered separately. These effects were consistently observed when averaging over entire sessions, as well as specifically following events of particular social importance, including mutual eye contact and mutual reward receipt. Furthermore, attention to various facial regions was differentially modulated depending on social context. Using the Allen Institute's transcriptional atlas, we further established the colocalization of μ-opioid and κ-opioid receptor genes and OT genes at the OT-releasing sites in the human brain. These data across monkeys and humans support a regulatory relationship between the OT and opioid systems and suggest that administering OT under opioid antagonism may boost the therapeutic efficacy of OT for enhancing social cognition.

oxytocin | opioid antagonist | naloxone | OXTR | OPRM1

The efficacy of oxytocin (OT) in improving social abilities is under debate, largely due to frequently observed weak effect sizes and problems with replicability (1–3). Clinical trials of OT in autistic patients are ongoing, yet several studies have produced inconclusive results (4–8), demanding improvements to the efficacy and reliability of OT-based therapeutics. One strategy is to take advantage of existing physiological pathways in the brain that regulate OT activity to combinatorially enhance the oxytocinergic effects on social functions. In this regard, a promising candidate is the opioid system.

In addition to the evolutionarily conserved OT system (9), the opioid system has been implicated in regulating social behavior. Excessive opioid activity in the brain has been discussed with respect to the development of early childhood autism (10). Abnormalities in central opioid levels have been observed in some individuals with autism, and clinical trials with predominantly μ-opioid blockers, such as naltrexone or naloxone (NAL), have yielded promising results in ameliorating both social and nonsocial deficits (11). Specifically, μ-opioid receptors have been studied in relation to reward, emotion, and behavior in the social domain (12) and are strongly expressed in reward-related regions of the primate brain (13). In rhesus macaques, carrying the G allele of the μ-opioid receptor gene *OPRM1*, compared with homozygous C alleles, is associated with stronger maternal attachment in infants (14) and more effective prevention of infant separation in mothers (15). Additionally, opioid agonists, such as morphine, decrease physical contact between social partners, whereas NAL administration increases solicitation for social contact, such as grooming and proximity (16–19).

The physiological relationship between the opioid and OT systems has been firmly established (20). Opioids directly inhibit OT secretion in mammals through action in the posterior pituitary and the hypothalamus (21, 22). Opioids not only inhibit OT release from the axon terminal in the posterior pituitary but also suppress the functional activity of OT neurons via opioid action on their cell bodies in the hypothalamus (23, 24). The chronic administration of morphine, a prototypical μ-opioid receptor agonist, also influences both the synthesis and secretion of OT (25). Despite the similar synthesis location of OT and vasopressin in the magnocellular neurons of the hypothalamus (21), opioids selectively regulate release of OT rather than vasopressin (22). Supporting this dissociation, endogenous opioid inhibition triggers central OT, but not vasopressin, release (26), and the high-affinity μ-opioid receptor antagonist NAL strongly drives OT, but not vasopressin, release from the posterior pituitary (22). Furthermore, during parturition, endogenous opioids control the release of OT both into blood and the brain in a tightly coordinated manner (26). Enhancing opioidergic tone with morphine severely delays the course of parturition, accompanied by a reduced level of circulating OT, whereas attenuating opioidergic tone with NAL acutely increases the speed of parturition by greatly elevating OT levels, reversing this delay (27–29). Similarly, the inhibition of OT secretion from neural tissues by morphine underlies the mechanism by which morphine disrupts milk ejection in lactation (30, 31).

Exploiting the regulatory relationship between the opioid and OT systems in the brain, we tested here whether administering OT

Significance

In the past decade, there has been an increase in studies using oxytocin (OT) for improving social cognition, but results have been inconsistent. In this study, we took advantage of the physiological relationship between the opioid and OT systems and tested the benefit of administering OT under simultaneously induced opioid antagonism during dyadic gaze interactions. Coadministration of OT and opioid blocker leads to supralinear enhancement of prolonged and selective attention to a live partner and increases interactive gaze after critical social events. Furthermore, we provide neurogenetic evidence in the human brain supporting the interaction between specific opioid receptor genes and the genes for OT processing. Our results suggest a new avenue for amplifying the efficacy of OT in clinical populations.

Author contributions: O.D.M. and S.W.C.C. designed research; O.D.M., M.P., and M.T. performed research; M.P., K.M.A., and A.J.H. analyzed data; and O.D.M., M.P., K.M.A., A.J.H., and S.W.C.C. wrote the paper.

The authors declare no conflict of interest.

This article is a PNAS Direct Submission. K.M.G. is a guest editor invited by the Editorial Board.

Data deposition: The data and codes used in this paper are available and downloadable through GitHub (https://github.com/changlabneuro/OT_NAL).

[1]O.D.M. and M.P. contributed equally to this work.

[2]To whom correspondence should be addressed. Email: olga.dalmonte@yale.edu.

This article contains supporting information online at www.pnas.org/lookup/suppl/doi:10.1073/pnas.1702725114/-/DCSupplemental.

in the presence of opioid antagonism could effectively promote social behavior. First, using multiple experimental approaches in nonhuman primates, we tested whether coadministration of OT and NAL leads to supralinear enhancement of attention directed to others compared with the summed effects observed from OT or NAL administrated separately, a conservative indicator of the combinatorial benefit. Second, in human brain tissues, we examined the colocalization of the μ-opioid, κ-opioid, and δ-opioid receptor genes with the OT gene, as well as the OT receptor gene, across 190 brain regions to provide the transcriptional correspondence of different types of opioid receptors with OT-secreting cells and OT receptors.

Results

For testing the behavioral impact of combined delivery of OT and NAL, pairs of monkeys sat directly across from each other while the eye positions from both monkeys were simultaneously and continuously recorded (32) (Fig. S1 *A* and *B*). Using a pediatric nebulizer, one of the animals in a given pair received aerosolized drugs intranasally corresponding to one of the four pharmacology conditions: OT [24 international units (IU)], NAL (1 mg), saline (SAL), or the combination of OT (24 IU) and NAL (1 mg) together (OTNAL) (*SI Results*, *NAL Dose–Response Curve* and Figs. S1*C* and S2). Fixation density maps (Fig. 1 *A* and *B*) show clear effects of OTNAL that encompass an increase in fixations to the eyes with a relative decrease in fixations to the mouth (Fig. 1*A*), and those maps suggest a supralinear effect of OTNAL, as shown by an increase in fixations to the eyes after subtracting the effect of OT plus NAL (Fig. 1*B*). OTNAL was associated with an increased number of fixations to the face of a conspecific compared with the SAL or OT condition [Fig. 1*C*; $F(3,76) = 5.14$, $P = 0.003$ for main effect, $P = 0.005$ for OTNAL over SAL, $P = 0.073$ for OTNAL over NAL, $P = 0.007$ for OTNAL over OT, one-way ANOVA with Tukey–Kramer post hoc tests]. To determine whether the effects of OTNAL were supralinear for the conspecific's face, we directly compared the effects of OTNAL with the added effects of OT and NAL alone over SAL control (i.e., a supralinear effect would be indicated by data points reliably falling above the unity line when the OTNAL effects are plotted on the ordinate as a function of the summed effects of OT and NAL on the abscissa). OTNAL had a larger effect for attention to the face than the added effects of OT and NAL alone [Fig. 1*D*; $t(19) = 2.42$, $P = 0.026$, paired-sample t test], with the effect size of OTNAL being correlated with the added effect sizes of OT and NAL alone ($r^2 = 0.33$, $P = 0.008$; linear regression). Furthermore, the OTNAL condition was associated with increased frequency of fixations to the eyes of a conspecific compared with the SAL or OT condition [Fig. 1*E*; $F(3,76) = 5.87$, $P = 0.004$ for main effect, $P = 0.004$ for OTNAL over SAL, $P = 0.069$ for OTNAL over NAL, $P = 0.022$ for OTNAL over OT], again with a supralinear pattern [Fig. 1*F*; $t(19) = 1.94$, $P = 0.067$]. This effect size of OTNAL was also correlated with the added effect sizes of OT and NAL alone (for eyes: $r^2 = 0.29$, $P = 0.014$). Critically, both for the face (Fig. S3*A*) and for the eyes (Fig. S3*B*), we found no significant modulation of fixation duration for any drug condition relative to SAL, indicating that there was no tradeoff between fixation frequency and fixation duration with respect to our observed effects, and that the effects were specific to increasing fixation frequency across all behavioral sessions to both the face and eyes. Additionally, the supralinear effects of OTNAL cannot be explained by a nonspecific increase in arousal, because the total count of fixations in the OTNAL condition was, in fact, not higher than in the SAL, NAL, or OT conditions (all $P > 0.05$, one-way ANOVA with Tukey–Kramer post hoc tests). Finally, in reference to previous literature documenting the effects of OT in social attention (33, 34), OT overall increased fixations to the eyes compared with SAL in this real-life dyadic setting [Fig. 1*E*; $t(19) = 1.63$, $P = 0.059$, paired-sample t test], although the effect was marginal.

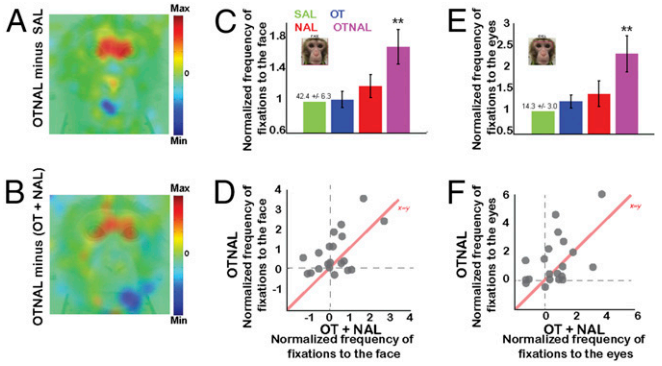

Fig. 1. Combined delivery of OT and NAL results in a supralinear enhancement of overall attention to the face and eyes of a conspecific. (*A*) Averaged heat map showing gaze fixations in the OTNAL condition over the SAL condition. (*B*) Averaged heat map showing fixations in the OTNAL condition over the summed effects of OT and NAL administered independently, demonstrating the supralinear effects. (*C*) Overall frequency of gaze fixations to the face of a conspecific in the OT (blue), NAL (red), and OTNAL (purple) conditions, normalized by the SAL (green) condition. (*D*) Effect size of OTNAL compared with the summed effect size of OT and NAL administered independently. (*E* and *F*) Overall frequency of gaze fixations to the eyes of a conspecific in the same format as in *C* and *D*. $^{**}P < 0.01$ over SAL condition, one-way ANOVA with Tukey–Kramer post hoc tests for multiple comparisons.

Gaze interactions are by nature dynamic and contingent between interacting agents. Following our pharmacological manipulations, we examined differences in gaze patterns focusing on time periods following mutual eye contact as instances of particular social importance (35–37). Following mutual eye contact, only OTNAL strongly increased attention to the conspecific (Fig. 2*A*; $P < 0.01$, permutation test). In fact, neither OT nor NAL administered alone had a significant effect in increasing attention to the conspecific following mutual eye contact compared with SAL (both $P > 0.05$, permutation tests). Notably, when comparing the effects of drugs following mutual eye contact, the resulting gaze patterns were again supralinear [Fig. 2*B*; $t(19) = 2.88$, $P = 0.010$, paired-sample t test]. We next tested whether the effects of OTNAL were specific to the periods following mutual eye contact as opposed to the periods following looking at the conspecific's eyes when the conspecifics were looking elsewhere than the partner's eyes. Following these instances of nonmutual eye contact, no significant results were observed for any pharmacological manipulation using the identical approach (Fig. 2*C*; all $P > 0.05$, permutation tests), indicating that the differences observed in the OTNAL condition selectively occurred during time periods of heightened social relevance. These effects were also observed to be specific to the eye region of interest (ROI), because gaze position returning to the mouth ROI after mutual eye contact, as well as after mutual gaze to the mouth of the conspecific, was not significantly affected by any pharmacological manipulation (Fig. S4 *A* and *B*; all $P > 0.05$, permutation tests).

During social interactions, attention can be allocated differentially between interacting individuals depending on the context. For example, a mutually beneficial event is particularly salient to social species living in large groups like macaques and humans, and such a prioritized behavioral relevance may be a foundational component guiding complex social interactions, such as coordinating with one another to obtain mutual benefits (38). Given the supralinear effects of OTNAL following mutual eye contact, we hypothesized similar combinatorial effects of OTNAL following mutual reward receipt by manipulating the receipt of mutual juice rewards during gaze interactions (Fig. S1*B*). Gaze frequency to the face of the conspecific was only significant in the OTNAL condition (Fig. 3*A*; $P < 0.001$, permutation test). Notably, these effects were again supralinear following mutual reward for OTNAL

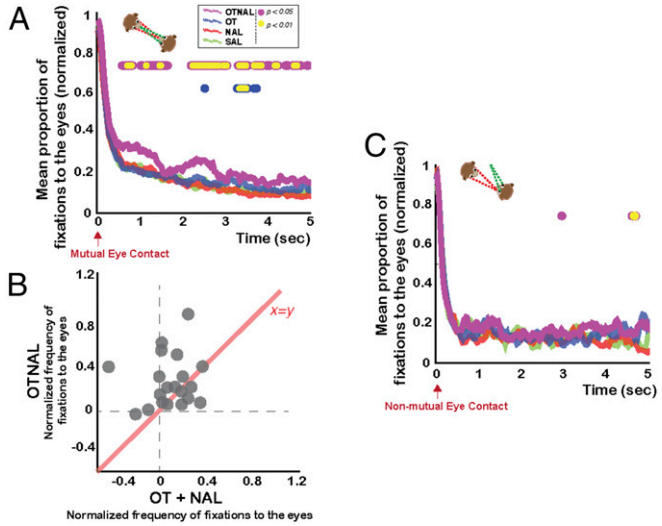

Fig. 2. Supralinear enhancements of dynamic gaze interactions following mutual eye contact by OTNAL. (*A*) Peristimulus time histograms (PSTHs), aligned to mutual eye contact, show the proportion of looking at the eyes following mutual eye contact in SAL (green), OT (blue), NAL (red), and OTNAL (purple) conditions. Horizontal marks indicate 10-ms time bins with significant differences ($P < 0.05$, OT over SAL, blue; $P < 0.05$, OTNAL over SAL, purple; $P < 0.01$, yellow; paired-sample *t* tests). (*B*) Effects size of OTNAL compared with the added effect size of OT and NAL alone for 0.5–3 s after mutual eye contact. (*C*) PSTH aligned to nonmutual eye contact in the same format as in *A*.

compared with the summed effects of OT and NAL, with a positive correlation between them [Fig. 3*B*; $t(19) = 2.14$, $P = 0.046$, paired-sample *t* test; $r^2 = 0.25$, $P = 0.023$, linear regression]. By contrast, when no reward was delivered to either animal, no modulations in gaze behaviors were found across all conditions (Fig. 3*C*; all $P > 0.05$, permutation tests), indicating that OTNAL also supralinearly influenced social gaze dynamics following mutually beneficial events.

Across mutual eye contact (Fig. 2) and mutual reward receipt (Fig. 3), the supralinear effects of OTNAL were driven by the most socially relevant features within the face of the conspecific, depending on the context of a given interactive event. Although the differences in gaze patterns following mutual eye contact in the OTNAL condition were specifically driven by returning gaze to the eye ROI (Fig. 2*A* and Fig. S4), the differences following mutual reward were specifically driven by attention to the mouth ROI (Fig. S5). Therefore, the supralinear effects of OTNAL are selective in that they were exerted by the most relevant features within the face of the conspecific depending on the interactive context.

Although the number of males and females tested in our study is underpowered for fully exploring potential sex difference, when we analyzed fixation frequency to the face (Fig. S6*A*) and eyes (Fig. S6*B*) over entire behavioral sessions, as well as gaze dynamics to the conspecific following mutual eye contact (Fig. S6*C*) and mutual reward (Fig. S6*D*), we found no significant effect of sex. Together, these results show that, within our limited sample size, drug effects are observed indistinguishably across both sexes.

We next identified potential brain regions underlying the facilitatory effects of opioid antagonism on OT in the human brain. We examined colocalization of gene expression patterns for the OT gene (*OXT*); OT receptor gene (*OXTR*); and μ-opioid (*OPRM1*), κ-opioid (*OPRK1*), and δ-opioid (*OPRD1*) receptor subtypes, using averaged microarray expression data of six postmortem donors from the Allen Human Brain Atlas. Available data included 190 regions containing samples from at least four donors (39). Transcription of the *OXT* was most pronounced in 10 regions displaying expression ≥1 SD above the region-wise mean [Fig. 4*A*; lateral hypothalamic area, tuberal region (LHT); paraventricular nucleus of the hypothalamus (PVH); supraoptic nucleus (SO); dorsomedial hypothalamic nucleus; lateral hypothalamic area, anterior region; lateral hypothalamic area, medial region; ventral hypothalamic area, medial region; perifornical nucleus; posterior hypothalamic area; and preoptic region].

Comparing the relative expression of *OPRM1*, *OPRK1*, and *OPRD1* among the 10 highest *OXT*-enriched regions responsible for endogenous OT release, we found significant main effects of opioid receptor subtype in each region (statistics are given below for three regions, and statistics for seven regions are given in the legend for Fig. S7). In all of these *OXT*-enriched regions, *OPRM1* and *OPRK1* displayed significantly greater expression than *OPRD1* (Fig. 4*B* and Fig. S7). The effects of opioid receptor subtype were particularly pronounced in the three regions with greatest *OXT* expression: LHT [$F(1,3) = 54.64$, $P = 0.005$ for main effect, $P = 0.002$ for μ over δ, $P = 0.002$ for κ over δ, $P = 0.691$ for μ over κ, one-way within-subjects ANOVA with Benjamini–Hochberg corrected post hoc tests)], PVH [$F(1,4) = 39.05$, $P = 0.003$ for main effect, $P < 0.001$ for μ over δ, $P < 0.001$ for κ over δ, $P = 0.201$ for μ over κ], and SO [$F(1,4) = 97.15$, $P < 0.001$ for main effect, $P < 0.001$ for μ over δ, $P < 0.001$ for κ over δ, $P = 0.005$ for μ over κ]. Robust above-average expression of *OPRM1* and *OPRK1* genes, but not *OPRD1*, was observed in all 10 *OXT*-enriched regions (Fig. 4*C*). Notably, the expression levels for *OPRM1* and *OXT* in the 10 *OXT*-enriched regions were correlated [$r(8) = 0.88$, $P < 0.001$, Pearson's correlation; Fig. 4*C*], whereas there were no such correlations for *OPRK1* [$r(8) = 0.15$, $P = 0.673$] and *OPRD1* [$r(8) = -0.17$, $P = 0.632$], insinuating a tighter coupling between *OXT* and *OPRM1*. Moreover, we also reliably observed above-average expression of *OXTR* in the *OXT*-enriched regions (Fig. 4*A* and Fig. S8), suggesting a regional colocalization of *OXT*, *OXTR*, *OPMR1*, and

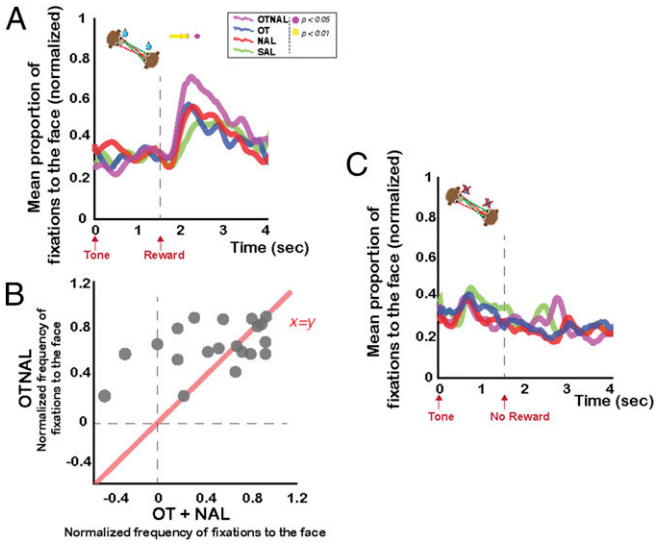

Fig. 3. Supralinear enhancements of dynamic gaze interactions following mutual reward by OTNAL. (*A*) PSTH shows the proportion of looking at the face following a tone predicting mutual reward in SAL (green), OT (blue), NAL (red), and OTNAL (purple) conditions. Reward occurred simultaneously for both monkeys 1.5 s after an unpredictable auditory tone. Horizontal marks indicate 10-ms time bins with significant differences ($P < 0.05$, OTNAL over SAL, purple; $P < 0.01$, yellow; paired-sample *t* tests). (*B*) Effects size of OTNAL versus the summed effect size of OT and NAL alone for 1.5–3.5 s after tone. (*C*) PSTH aligned to tones that did not result in reward to either monkey in the same format as in *A*. No 10-ms time bin for any drug condition was significantly higher than SAL (all $P > 0.05$, paired-sample *t* tests).

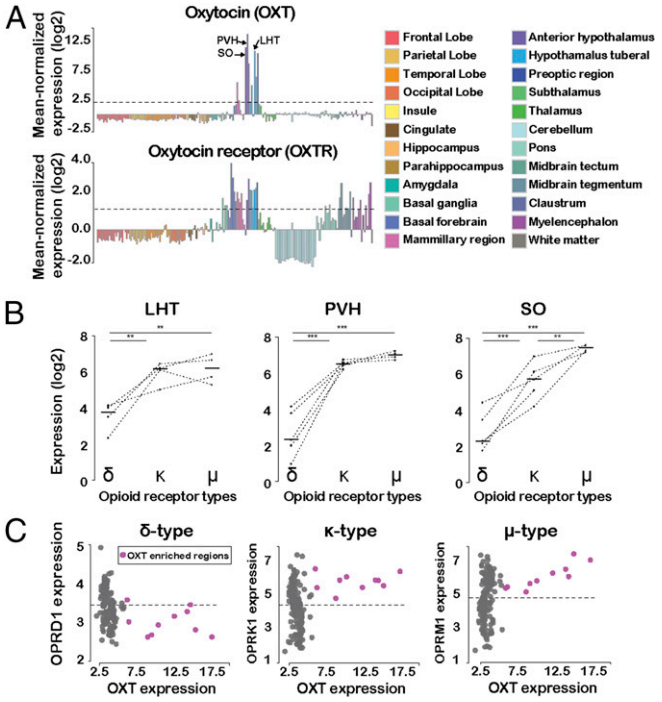

Fig. 4. Genes encoding μ-opioid and κ-opioid, but not δ-opioid, receptors display above-average expression in OT-enriched regions. (*A*) Microarray expression of *OXT* and *OXTR* from 190 regions averaged across six postmortem human brains from the Allen Human Brain Atlas (AHBA). Ten tissue samples displayed OXT expression 1 SD above the mean: LHT, PVH, SO, dorsomedial hypothalamic nucleus (DMH), lateral hypothalamic area, anterior region (LHA), lateral hypothalamic area, medial region (LHM), ventral hypothalamic area, medial region (VHM), perifornical nucleus (PeF), posterior hypothalamic area (PHA), and preoptic region (PrOR). (*B*) μ-Opioid and κ-opioid receptor genes are expressed significantly more than δ-opioid receptor genes across the top three *OXT*-enriched regions (data from the remaining seven *OXT*-enriched regions are shown in Fig. S7). Each line connects samples from the same donor. Different numbers of lines are due to nonuniform sampling across the six AHBA donors. The horizontal ticks indicate the mean of different donors. (*C*) Across all 190 regions, μ-opioid and κ-opioid receptors displayed above-average expression within the eight *OXT*-enriched samples. $*P < 0.05$, $**P < 0.01$, $***P < 0.001$.

OPRK1. Taken together, these results indicate the preferential role of μ-opioid and κ-opioid receptor subtypes in OT-secreting brain regions.

Discussion

In this preclinical pharmacological investigation, we report an alternate avenue for amplifying the efficacy of OT in directing selective and prolonged attention to social cues by administering OT under opioid antagonism. The supralinear effects of OTNAL were driven by mutually engaged events (mutual eye contact and mutual reward receipt) and resulted in directing selective attention to socially relevant features (eyes and mouth, respectively). The potential benefit of coadministering OT with NAL is supported by the mechanistic link between the inhibition of opioid processing and increase in OT release from the posterior pituitary (22), as well as the colocalization of the expressed OT receptor and μ-opioid and κ-opioid receptor genes at the primary OT-releasing sites in the human brain.

Because the opioid system involves at least three principal receptor types (μ-opioid, κ-opioid, and δ-opioid receptors), determining which specific receptor subtypes mediate the effect of endogenous opioids on the OT system is of interest. Bicknell and Leng (40) examined the effects of a range of opioid agonists and antagonists with different relative selectivity toward opioid receptor subclasses on the secretion of OT from the isolated posterior pituitary. The authors reported that NAL, the relatively μ-selective antagonist (41) used in our study, enhanced OT secretion by up to 90%. Douglas et al. (42) showed that in late pregnant rats, endogenous opioids inhibit OT neurons through μ-opioid receptors rather than κ-opioid receptors. Norbinaltorphimine, a specific κ-opioid receptor antagonist, did not increase neuronal activity or affect OT release in the SO, whereas NAL rapidly increased OT secretion (43, 44) and increased neuronal activity in the SO (42). Our analysis of human brain tissue indicates the colocalization of μ-opioid and κ-opioid receptor genes, but not δ-opioid receptor genes, and OT genes at the OT-releasing sites in the brain, including the SO, PVH, and LHT, but not in other cortical and subcortical regions. Based on NAL's much higher affinity for μ-type than for κ-type (greater than eightfold) and δ-type (>60-fold) receptors (45), the supralinear results of OTNAL here are likely driven most strongly by the OT-secreting cells expressing the μ-opioid receptor subtypes, as suggested from posterior pituitary as well as lactation and parturition studies (30, 31). This finding is consistent with the notion that OTNAL is amplifying the known OT effects on social attention associated with systemic OT manipulations, in which the functional specificity is likely to be localized to OT-sensitive brain regions following an enhancement of the oxytonergic tone of the brain. Taken together, these findings suggest that the effects of NAL are likely mediated by inhibition of μ-opioid and possibly also κ-opioid receptors, but not δ-opioid receptors.

We hypothesize that the supralinear effects of OTNAL results from elevations of endogenous OT toward a threshold that allows the brain to engage robustly in social functions. The supralinear effects of OTNAL may be due to simultaneous engagement of feedforward endogenous OT release from neurons with OT receptors (46), as well as the removal of opioid-mediated inhibition of OT release in OT neurons (27), resulting in overall higher endogenous OT levels that reach a threshold needed for social functions. Observational studies in patients with autism have shown that administration of an opioid antagonist could decrease self-injurious behavior, stereotypies, hyperactivity, and withdrawal, although increasing verbal production, social communication, proximity seeking, and eye contact (47–50). However, in the past decade, there has been a striking reduction in research using opioid antagonists as a means to ameliorate social deficits, whereas there has been a marked increase in studies testing the benefits of OT on social attention, although with inconclusive results. Our results indicate that combined administration of exogenous OT and NAL may improve the efficacy of pharmacological therapies to enhance social functions by leveraging endogenous OT release.

Materials and Methods

All procedures were approved by the Yale Institutional Animal Care and Use Committee and were in compliance with the Public Health Service's *Guide for the Care and Use of Laboratory Animals* (51).

Behavioral Tasks.

Live gaze interaction task. Two animals sat in front of each other with no task constraints while the eye positions of both animals were recorded simultaneously and continuously (Fig. S1*A*). Horizontal and vertical eye positions were sampled at 1,000 Hz using two infrared eye monitor camera systems (Eyelink; SR Research). The two monkeys were positioned 62 cm apart from one another, with the top of each monkey's head at 76 cm from the floor. Before starting to record gaze behavior, each animal underwent a systematic calibration procedure (details are provided in *SI Materials and Methods*, *Behavioral Tasks* and ref. 32). During the calibration and until the beginning of each session, the two animals had no visual access to each other, with a screen fully separating the view of both animals. The screen was lifted at the start of each session, marking the beginning of the live gaze interaction task. Each session lasted 3 min, for a total of eight sessions each day, with a 3-min break between sessions with no visual access. One of the two animals in a given pair was administered a drug via nebulizer (details are provided in *SI Materials and Methods*, *Subjects*) corresponding to one of the four pharmacology conditions: OT (24 IU), NAL (1 mg), SAL,

or the combination of OT (24 IU) and NAL (1 mg) together (OTNAL). Behavioral testing began 30 min after each treatment and lasted for about 45 min. A total of five animals (three males and two females) with between three and five distinct conspecifics (total of 20 pairs) participated in all four pharmacology conditions. We collected 640 sessions in total: 32 sessions for each drug condition per subject.

Mutual reward task. Animals were placed in the same configuration as in the live gaze interaction task. In this task, two speakers (each speaker located by the chair of each monkey) and two juice tubes, one for each monkey, were added to the setup. An auditory tone was played at random time intervals (between 4 and 16 s). Following the tone, simultaneous juice rewards to both monkeys (0.5 mL) or no rewards to both monkeys could occur at equal probabilities after 1.5 s (Fig. S1*B*). Before and between these sessions, an occluder was placed between the animals. Similar to the live gaze interaction task, the eye movements of both animals were completely unconstrained, allowing for examination of naturalistic gaze patterns, and one of the two animals in a given pair was administered one of the four drugs via a nebulizer. Each session lasted 5 min, for a total of four sessions each day, with a 3-min break between sessions with no visual access. A total of five animals (three males and two females) with between three and five distinct conspecifics (total of 20 pairs) participated in all four drug conditions. We collected 320 sessions in total: 16 sessions for each drug condition per subject. The mutual reward task was always performed after the live gaze interaction task, ∼75 min after administration of each drug, and lasted for about 30 min.

Statistical Analysis.

Fixation analyses over entire sessions. Fixations to the defined eye regions were first obtained for each monkey, as were the fixations to the face and total fixations occurring in the setup for the SAL, NAL, OT, and OTNAL drug conditions. Fixations to the eye region and overall face were normalized in the NAL, OT, and OTNAL conditions by the SAL baseline within pairs, and pairs were then averaged within each drug condition (Fig. 1). These values were compared with a one-way ANOVA (with condition as a factor) and subsequent multiple comparison tests (Tukey–Kramer post hoc tests). For measures of overall attention to the eyes and face of a conspecific, supralinearity was determined by comparing the effects of OTNAL with the summed effects of OT and NAL alone with a paired-sample *t* test. Correlation between these two measures was also evaluated via linear regression, with significance determined by an *F* test for the model.

Dynamic gaze analyses. To measure gaze dynamics following mutual eye contact, we identified mutual eye contact events in which both animals initiated eye contact within a window measuring a 7.7° × 3.8° visual angle. A 5-s window after each instance of mutual eye contact was examined to identify when and how long the monkey looked back into the eyes of the conspecific. Similarly, a 4-s window was taken after each tone that eventually predicted mutual reward. These 5-s and 4-s windows were chosen empirically based on the observation that looking behaviors return to a rough baseline, with no significant differences between drug groups observed after these periods (Figs. 2 and 3). We used 10-ms bins and created binary datasets to characterize whether the animal was looking at the face of the conspecific within each bin. If a given animal looked back into the face of a conspecific at any time within a given 10-ms bin, that bin was given a value of 1. Otherwise, that bin was given a value of 0. Total amount of return viewing was summed over all instances of mutual eye contact on a given day of testing, normalized by the bin with the highest instance of returning gaze, and then averaged across pairs to compare quantitatively across drug conditions.

To analyze differences between drug groups, we first performed *t* tests to compare values at all bins within the 5-s periods after mutual eye contact. Windows of activity were defined in which gaze behavior between the two groups diverged (500–3,000 ms for mutual eye contact and 1,500–3,500 ms for mutual reward). Significant differences of drug conditions over the SAL baseline within these windows were determined with a permutation test by shuffling the data 1,000 times and randomly assigning the data from each monkey an identity in one of the groups (SAL baseline or a given drug group) being compared in each condition. The data were then averaged and compared, with a discrete value being obtained as the maximum difference between groups in some bin within the defined window. The permutated values were then sequentially ordered for determining threshold values for significance. To determine whether our findings were specific to periods following interactive events, we aligned to nonmutual eye contact and tones after which reward was not administered to either monkey. Analyses identical to those analyses mentioned above were applied.

To test whether discrete areas of the face were driving these differences in each condition, we redefined the ROIs for determining whether or not animals looked back at the conspecific. For mutual eye contact, we conducted two control analyses. The first control analysis retained mutual eye contact events, but instead measured attention to the mouth of the conspecific following eye contact. The second control analysis determined attention to the mouth of the conspecific following simultaneous gaze to the mouth ROI. The mouth region was defined with a window measuring 5.3° × 8.0° visual angle. We then repeated the same analyses as mentioned above for these controls. For mutual reward receipt, we examined the eye and mouth individually to determine what smaller ROIs were driving overall attention to the face. After defining these two new ROIs, analyses identical to those analyses mentioned above were again applied.

When comparing the effects of OT and NAL alone with the OTNAL combination condition, supralinearity was determined by first quantifying the effect sizes for OT, NAL, and OTNAL over the SAL baseline for mutual eye contact and mutual reward events. This quantification analysis was accomplished by searching in our 500- to 3,000-ms window of activity for mutual eye contact and in our 1,500- to 3,500-ms window of activity for mutual reward for the time bin in which OTNAL had a maximal effect over SAL. This effect of OTNAL was then compared with the added maximal effects of the separate OT and NAL conditions over SAL with a paired-sample *t* test to determine significance. Correlation between these two measures was also evaluated via linear regression, with significance determined by the *F* test for the model.

Human neurogenetics analysis. Six postmortem human brains from the Allen Human Brain Atlas (39) were analyzed and downloaded after updated normalization procedures implemented by the Allen Institute in March 2013. For the mRNA dataset, the data can be downloaded directly from the Allen Brain Atlas (brain-map.org/). Each individual donor's dataset includes normalized microarray expression data (help.brain-map.org/display/humanbrain/documentation/). Microarray probes without an Entrez ID were not examined. Probe selection was conducted according to the analysis of Miller et al. (52) to analyze probes that most reliably align to RNA-sequencing values, resulting in 20,736 unique gene probes. To prevent biased expression values due to sparse sampling across the six donors, only regions that were sampled in at least four donors were examined. The resulting 190 unique regions and their ontological assignment to each category in Fig. 4 and Figs. S7 and S8 are documented in Table S1. If more than one sample was present in a given region in a given donor, the microarray expression values were averaged.

To identify regions that most express *OXT*, microarray data for each of the 190 regions were averaged across subjects. Regions falling 1 SD above the z-transformed mean were identified as "*OXT*-enriched" (Fig. 4 and Figs. S7 and S8). Differences in expression of the μ-opioid (*OPRM1*), κ-opioid (*OPRK1*), and σ-opioid (*OPRD1*) receptor subtypes within each *OXT*-enriched region were then examined using a within-subject one-way ANOVA (with opioid receptor subtype as a factor) and subsequent multiple comparison tests (false discovery rate Benjamini–Hochberg-corrected). Finally, we examined whether *OPRM1*, *OPRK1*, and *OPRD1*, as well as *OXTR*, displayed above-average expression within *OXT*-enriched regions by plotting their region-wise microarray expression values against the microarray expression values of OXT.

ACKNOWLEDGMENTS. We thank A. Nair for her helpful suggestions and T. Stavropoulos for his technical assistance. This work was supported by the Simons Foundation Autism Research Initiative (Grant 365029 to S.W.C.C.), an Alfred P. Sloan Foundation Neuroscience Fellowship (FG-2015-66028 to S.W.C.C.), a Teresa Seessel Endowed Postdoctoral Fellowship (to O.D.M.), a Natural Sciences and Engineering Council of Canada Predoctoral Fellowship (PGSD3-471313-2015 to M.P.), the National Institute of Mental Health (Grant R01MH110750 to S.W.C.C. and Grant K01MH099232 to A.J.H.), and the National Science Foundation (Grant DGE-1122492 to K.M.A.).

1. Bartz J, et al. (2011) Oxytocin can hinder trust and cooperation in borderline personality disorder. *Soc Cogn Affect Neurosci* 6:556–563.
2. Walum H, Waldman ID, Young LJ (2016) Statistical and methodological considerations for the interpretation of intranasal oxytocin studies. *Biol Psychiatry* 79:251–257.
3. Leng G, Ludwig M (2016) Intranasal oxytocin: Myths and delusions. *Biol Psychiatry* 79: 243–250.
4. Anagnostou E, et al. (2014) Intranasal oxytocin in the treatment of autism spectrum disorders: A review of literature and early safety and efficacy data in youth. *Brain Res* 1580:188–198.
5. Yatawara CJ, Einfeld SL, Hickie IB, Davenport TA, Guastella AJ (2016) The effect of oxytocin nasal spray on social interaction deficits observed in young children with autism: A randomized clinical crossover trial. *Mol Psychiatry* 21:1225–1231.
6. Anagnostou E, et al. (2012) Intranasal oxytocin versus placebo in the treatment of adults with autism spectrum disorders: A randomized controlled trial. *Mol Autism* 3:16.
7. Preckel K, Kanske P, Singer T, Paulus FM, Krach S (2016) Clinical trial of modulatory effects of oxytocin treatment on higher-order social cognition in autism spectrum disorder: A randomized, placebo-controlled, double-blind and crossover trial. *BMC Psychiatry* 16:329.

8. Guastella AJ, et al. (2015) The effects of a course of intranasal oxytocin on social behaviors in youth diagnosed with autism spectrum disorders: A randomized controlled trial. *J Child Psychol Psychiatry* 56:444–452.
9. Carter CS (2014) Oxytocin pathways and the evolution of human behavior. *Annu Rev Psychol* 65:17–39.
10. Panksepp J (1979) A neurochemical theory of autism. *Trends Neurosci* 2:174–177.
11. Roy A, Roy M, Deb S, Unwin G, Roy A (2015) Are opioid antagonists effective in attenuating the core symptoms of autism spectrum conditions in children: A systematic review. *J Intellect Disabil Res* 59:293–306.
12. Resendez SL, et al. (2013) μ-Opioid receptors within subregions of the striatum mediate pair bond formation through parallel yet distinct reward mechanisms. *J Neurosci* 33:9140–9149.
13. Ragen BJ, Freeman SM, Laredo SA, Mendoza SP, Bales KL (2015) μ and κ opioid receptor distribution in the monogamous titi monkey (Callicebus cupreus): Implications for social behavior and endocrine functioning. *Neuroscience* 290:421–434.
14. Barr CS, et al. (2008) Variation at the mu-opioid receptor gene (OPRM1) influences attachment behavior in infant primates. *Proc Natl Acad Sci USA* 105:5277–5281.
15. Higham JP, et al. (2011) Mu-opioid receptor (OPRM1) variation, oxytocin levels and maternal attachment in free-ranging rhesus macaques Macaca mulatta. *Behav Neurosci* 125:131–136.
16. Kalin NH, Shelton SE, Barksdale CM (1988) Opiate modulation of separation-induced distress in non-human primates. *Brain Res* 440:285–292.
17. Fabre-Nys C, Meller RE, Keverne EB (1982) Opiate antagonists stimulate affiliative behaviour in monkeys. *Pharmacol Biochem Behav* 16:653–659.
18. Martel FL, Nevison CM, Simpson MJ, Keverne EB (1995) Effects of opioid receptor blockade on the social behavior of rhesus monkeys living in large family groups. *Dev Psychobiol* 28:71–84.
19. Keverne EB, Martensz ND, Tuite B (1989) Beta-endorphin concentrations in cerebrospinal fluid of monkeys are influenced by grooming relationships. *Psychoneuroendocrinology* 14: 155–161.
20. Vuong C, Van Uum SH, O'Dell LE, Lutfy K, Friedman TC (2010) The effects of opioids and opioid analogs on animal and human endocrine systems. *Endocr Rev* 31:98–132.
21. Vandesande F, Dierickx K (1975) Identification of the vasopressin producing and of the oxytocin producing neurons in the hypothalamic magnocellular neurosecretory system of the rat. *Cell Tissue Res* 164:153–162.
22. Bicknell R, Leng G (1982) Endogenous opiates regulate oxytocin but not vasopressin secretion from the neurohypophysis. *Nature* 298:161–162.
23. Pumford KM, Leng G, Russell JA (1991) Morphine actions on supraoptic oxytocin neurones in anaesthetized rats: Tolerance after i.c.v. morphine infusion. *J Physiol* 440: 437–454.
24. Bicknell RJ, Ingram CD, Leng G (1983) Oxytocin release is inhibited by opiates from the neural lobe, not those from the intermediate lobe. *Neurosci Lett* 43:227–230.
25. You ZD, Li JH, Song CY, Wang CH, Lu CL (2000) Chronic morphine treatment inhibits oxytocin synthesis in rats. *Neuroreport* 11:3113–3116.
26. Neumann I, Russell JA, Wolff B, Landgraf R (1991) Naloxone increases the release of oxytocin, but not vasopressin, within limbic brain areas of conscious parturient rats: A push-pull perfusion study. *Neuroendocrinology* 54:545–551.
27. Bicknell RJ, et al. (1988) Hypothalamic opioid mechanisms controlling oxytocin neurones during parturition. *Brain Res Bull* 20:743–749.
28. Leng G, et al. (1988) Endogenous opioid actions and effects of environmental disturbance on parturition and oxytocin secretion in rats. *J Reprod Fertil* 84:345–356.
29. Bicknell RJ, Leng G, Lincoln DW, Russell JA (1988) Naloxone excites oxytocin neurones in the supraoptic nucleus of lactating rats after chronic morphine treatment. *J Physiol* 396:297–317.
30. Clarke G, Wood P, Merrick L, Lincoln D (1979) Opiate inhibition of peptide release from the neurohumoral terminals of hypothalamic neurons. *Nature* 282:746–748.
31. Rayner VC, Robinson IC, Russell JA (1988) Chronic intracerebroventricular morphine and lactation in rats: Dependence and tolerance in relation to oxytocin neurones. *J Physiol* 396:319–347.
32. Dal Monte O, Piva M, Morris JA, Chang SW (2016) Live interaction distinctively shapes social gaze dynamics in rhesus macaques. *J Neurophysiol* 116:1626–1643.
33. Chang SW, Platt ML (2014) Oxytocin and social cognition in rhesus macaques: Implications for understanding and treating human psychopathology. *Brain Res* 1580: 57–68.
34. Guastella AJ, MacLeod C (2012) A critical review of the influence of oxytocin nasal spray on social cognition in humans: Evidence and future directions. *Horm Behav* 61: 410–418.
35. Wilms M, et al. (2010) It's in your eyes–using gaze-contingent stimuli to create truly interactive paradigms for social cognitive and affective neuroscience. *Soc Cogn Affect Neurosci* 5:98–107.
36. Schilbach L (2015) Eye to eye, face to face and brain to brain: Novel approaches to study the behavioral dynamics and neural mechanisms of social interactions. *Curr Opin Behav Sci* 3:130–135.
37. Emery NJ (2000) The eyes have it: The neuroethology, function and evolution of social gaze. *Neurosci Biobehav Rev* 24:581–604.
38. Mitani JC, Call J, Kappeler PM, Palombit RA, Silk JB (2012) *The Evolution of Primate Societies* (Univ of Chicago Press, Chicago).
39. Hawrylycz MJ, et al. (2012) An anatomically comprehensive atlas of the adult human brain transcriptome. *Nature* 489:391–399.
40. Bicknell RJ, Leng G (1982) Endogenous opiates regulate oxytocin but not vasopressin secretion from the neurohypophysis. *Nature* 298:161–162.
41. Lutz-Bucher B, Koch B (1980) Evidence for a direct inhibitory effect of morphine on the secretion of posterior pituitary hormones. *Eur J Pharmacol* 66:375–378.
42. Douglas AJ, et al. (1995) Central endogenous opioid inhibition of supraoptic oxytocin neurons in pregnant rats. *J Neurosci* 15:5049–5057.
43. Hartman RD, Rosella-Dampman LM, Emmert SE, Summy-Long JY (1986) Inhibition of release of neurohypophysial hormones by endogenous opioid peptides in pregnant and parturient rats. *Brain Res* 382:352–359.
44. Douglas AJ, Dye S, Leng G, Russell JA, Bicknell RJ (1993) Endogenous opioid regulation of oxytocin secretion through pregnancy in the rat. *J Neuroendocrinol* 5: 307–314.
45. Codd EE, Shank RP, Schupsky JJ, Raffa RB (1995) Serotonin and norepinephrine uptake inhibiting activity of centrally acting analgesics: Structural determinants and role in antinociception. *J Pharmacol Exp Ther* 274:1263–1270.
46. Bakermans-Kranenburg MJ, van I Jzendoorn MH (2013) Sniffing around oxytocin: review and meta-analyses of trials in healthy and clinical groups with implications for pharmacotherapy. *Transl Psychiatry* 3:e258.
47. Bouvard MP, et al. (1995) Low-dose naltrexone effects on plasma chemistries and clinical symptoms in autism: A double-blind, placebo-controlled study. *Psychiatry Res* 58:191–201.
48. Campbell M, et al. (1993) Naltrexone in autistic children: Behavioral symptoms and attentional learning. *J Am Acad Child Adolesc Psychiatry* 32:1283–1291.
49. Leboyer M, et al. (1992) Brief report: A double-blind study of naltrexone in infantile autism. *J Autism Dev Disord* 22:309–319.
50. Williams PG, Allard A, Sears L, Dalrymple N, Bloom AS (2001) Brief report: Case reports on naltrexone use in children with autism: Controlled observations regarding benefits and practical issues of medication management. *J Autism Dev Disord* 31:103–108.
51. National Research Council (2011) *Guide for the Care and Use of Laboratory Animals* (National Academies Press, Washington, DC), 8th Ed.
52. Miller JA, et al. (2014) Improving reliability and absolute quantification of human brain microarray data by filtering and scaling probes using RNA-Seq. *BMC Genomics* 15:154.
53. Neumann ID, Maloumby R, Beiderbeck DI, Lukas M, Landgraf R (2013) Increased brain and plasma oxytocin after nasal and peripheral administration in rats and mice. *Psychoneuroendocrinology* 38:1985–1993.
54. Chang SW, Barter JW, Ebitz RB, Watson KK, Platt ML (2012) Inhaled oxytocin amplifies both vicarious reinforcement and self reinforcement in rhesus macaques (Macaca mulatta). *Proc Natl Acad Sci USA* 109:959–964.
55. Dal Monte O, Noble PL, Turchi J, Cummins A, Averbeck BB (2014) CSF and blood oxytocin concentration changes following intranasal delivery in macaque. *PLoS One* 9:e103677.
56. Brainard DH (1997) The psychophysics toolbox. *Spat Vis* 10:433–436.
57. Wermeling DP (2013) A response to the opioid overdose epidemic: Naloxone nasal spray. *Drug Deliv Transl Res* 3:63–74.
58. Wolfe TR, Bernstone T (2004) Intranasal drug delivery: An alternative to intravenous administration in selected emergency cases. *J Emerg Nurs* 30:141–147.
59. Sabzghabaee AM, Eizadi-Mood N, Yaraghi A, Zandifar S (2014) Naloxone therapy in opioid overdose patients: Intranasal or intravenous? A randomized clinical trial. *Arch Med Sci* 10:309–314.
60. Hussain A, Kimura R, Chong-Heng H, Kashihara T (1984) Nasal absorption of naloxone and buprenorphine in rats. *Int J Pharm* 21:233–237.
61. Middleton LS, Nuzzo PA, Lofwall MR, Moody DE, Walsh SL (2011) The pharmacodynamic and pharmacokinetic profile of intranasal crushed buprenorphine and buprenorphine/naloxone tablets in opioid abusers. *Addiction* 106:1460–1473.
62. Kerr D, Dietze P, Kelly AM (2008) Intranasal naloxone for the treatment of suspected heroin overdose. *Addiction* 103:379–386.
63. Wardle MC, Bershad AK, de Wit H (2016) Naltrexone alters the processing of social and emotional stimuli in healthy adults. *Soc Neurosci* 11:579–591.
64. Dal Monte O, Noble PL, Costa VD, Averbeck BB (2014) Oxytocin enhances attention to the eye region in rhesus monkeys. *Front Neurosci* 8:41.
65. Landman R, Sharma J, Sur M, Desimone R (2014) Effect of distracting faces on visual selective attention in the monkey. *Proc Natl Acad Sci USA* 111:18037–42.
66. Gamer M, Zurowski B, Büchel C (2010) Different amygdala subregions mediate valence-related and attentional effects of oxytocin in humans. *Proc Natl Acad Sci USA* 107:9400–9405.
67. Gamer M, Büchel C (2012) Oxytocin specifically enhances valence-dependent parasympathetic responses. *Psychoneuroendocrinology* 37:87–93.
68. MacDonald E, et al. (2011) A review of safety, side-effects and subjective reactions to intranasal oxytocin in human research. *Psychoneuroendocrinology* 36:1114–1126.
69. Campbell M, et al. (1990) Naltrexone in autistic children: A double-blind and placebo-controlled study. *Psychopharmacol Bull* 26:130–135.
70. Campbell M, et al. (1989) Naltrexone in autistic children: An acute open dose range tolerance trial. *J Am Acad Child Adolesc Psychiatry* 28:200–206.
71. Domes G, et al. (2013) Effects of intranasal oxytocin on the neural basis of face processing in autism spectrum disorder. *Biol Psychiatry* 74:164–171.
72. Merlin MA, et al. (2010) Intranasal naloxone delivery is an alternative to intravenous naloxone for opioid overdoses. *Am J Emerg Med* 28:296–303.
73. Walley AY, et al. (2013) Opioid overdose prevention with intranasal naloxone among people who take methadone. *J Subst Abuse Treat* 44:241–247.
74. Doe-Simkins M, Walley AY, Epstein A, Moyer P (2009) Saved by the nose: Bystander-administered intranasal naloxone hydrochloride for opioid overdose. *Am J Public Health* 99:788–791.

Supporting Information

Dal Monte et al. 10.1073/pnas.1702725114

SI Materials and Methods

Subjects.

Animals and surgical procedure. Nine adult rhesus macaques (*Macaca mulatta*) were involved in this study. Animals (six males and three females) were all housed together in a colony in either pairs or triads. Each animal was kept on a 12-h light/dark cycle and had access to food 24 h each day with controlled access to water during testing. Before testing began, each monkey received a surgically implanted head post (Crist Instruments, Gray Matter Research) for restraining its head while tracking eye positions. At the time of surgery, anesthesia was induced with ketamine hydrochloride (10 mg/kg i.m.) and maintained with isoflurane (1.0–3.0%, to effect). Aseptic procedures were used, and heart rate, respiration rate, blood pressure, expired CO_2, and body temperature were monitored throughout the procedure. Monkeys were allowed an additional 30–40 d of recovery after the implant surgery. All procedures were approved by the Yale Institutional Animal Care and Use Committee and were in compliance with the Public Health Service's *Guide for the Care and Use of Laboratory Animals* (51).

Pharmacological manipulations (nebulized intranasal administration). All of the tested subjects in this study received pharmacological manipulations through a pediatric nebulizer (PARI Baby Nebulizer; PARI Respiratory Equipment) with a cone-shaped facemask. The facemask, designed for canine anesthesia, was fitted entirely over the muzzle area, and the subject breathed freely through the nose for the duration of the dose administration. Before experimental sessions, monkeys were first incrementally habituated to the facemask and then to the nebulizer until they were completely relaxed during the procedure, which typically took about 3–5 d. This habituation procedure was performed with SAL. During both the habituation phase and the testing phase, the animals' heads were restrained to minimize movement and enhance administration reliability. Each of the different pharmacology manipulations tested (discussed below) was diluted to a volume of 2 mL using sterile SAL and was administered over the course of 8–10 min. In addition, experimental sessions were conducted at the same time of day to control for diurnal fluctuations. Behavioral testing began 30 min after each treatment, given that animal studies in both rodents (53) and nonhuman primate (54, 55) have shown central elevations of OT concentration after 30 min from intranasal administration. Finally, we used a within-subjects design so that each animal experienced all drug conditions with a randomized order on consecutive days of administration across animals.

Behavioral Tasks.

Calibration procedures for the live gaze interaction task and mutual reward task. We used the same gaze calibration procedures for studying dyadic gaze interactions reported by Dal Monte et al. (32). Before each experimental session, each of the two animals underwent a systematic calibration procedure. Subjects were required to fixate on a specific point at a specific time to estimate the viewing angle based on a temporarily placed screen (36 cm away from the subject's eyes, located exactly in middle distance between the two subjects). Stimuli were controlled by the Psychtoolbox and Eyelink toolbox in MATLAB (MathWorks) (56). The identical procedure was repeated for the second animal. For analysis purposes, we also determined where the animal was looking on a theoretical screen located further from the actual screen on which the animal was calibrated. With trigonometric corrections, the ROIs were identified and matched based on individual measurements of each monkey's face to the dimension of fixations as measured from the calibration screen. Fixations were then mapped in detail across the face of the conspecific (32).

Free-viewing task. Most studies and clinical applications of NAL have delivered NAL by the i.v., i.m., or s.c. route, with the i.v. route being the recommended route (57). Recently, the intranasal delivery method has been suggested as a route to administer NAL quickly in a needle-free system (58). It has been shown that the same dose of intranasal NAL is as effective as i.v. NAL in reversing effects on the central nervous system caused by opioid overdose in humans (59). Similarly, in rodents, the absorption of NAL through the nasal route has been found to be equivalent to the i.v. and intraduodenal routes (60). In humans, the pharmacodynamic profile of NAL intranasal administration has been investigated with different doses ranging from 0.5 to 2 mg (61). Today, the common dose used for NAL nasal spray in prehospital settings with heroin overdose is 2 mg (58, 62). Although increasing evidence points toward nasal spray as a reliable delivery route, no studies have investigated the effect of NAL on social behaviors in humans or nonhuman primates following intranasal administration. Therefore, to determine the optimal dosage of NAL for eliciting social effects, we completed a preliminary dose–response study of intranasal NAL (N7758; Sigma) administration in three animals (two male and one female adult rhesus monkeys) during the free-viewing task. On the day of the experiment, monkeys were transported in a primate chair from the colony room to the experimental room. After restraining their heads, doses of 0.5 mg, 1 mg, or 2 mg of NAL or sterile SAL were administered with a nebulizer in a 2-mL volume of sterile SAL. Behavioral testing began 30 min after each treatment and lasted for about 150 min. Monkeys first acquired and held a central fixation point for 150 ms, followed by freely viewing images for 15 s. During the 15-s period, monkeys were free to explore, or not explore, each face presented while an infrared eye-tracking camera continuously recorded their eye positions (Eyelink; SR Research). At the end of the 15-s presentation, a juice reward (0.3 mL) was delivered, regardless of the gaze pattern of the subject (Fig. S1*C*). Images were presented randomly, and monkeys saw an average of 132 ± 19 images per day. Each daily session used a different stimulus set. Each stimulus set contained 96 unique human and monkey faces (48 images each).

Statistical Analysis.

NAL dose–response curve. Although a recent paper has suggested that the opioid blocker naltrexone alters the processing of social and emotional stimuli in healthy subjects (63), no studies to date have provided a dose–response curve for the impact of intranasal NAL on social attention in either humans or nonhuman primates. We first conducted an independent pharmacology experiment to determine the optimal dose of NAL for directing attention to the face and eyes of conspecifics (1 mg) before the main testing sessions (as discussed above and shown in Figs. S1*C* and S2). For OT (O3251; Sigma), we chose the conventional dose of 24 IU used in both humans and nonhuman primates (34, 64). This dose, administered intranasally, has been shown in nonhuman primates to increase OT levels in cerebrospinal fluid significantly (54) and to modulate social behavior (65), as well as to affect brain activity (66) and phasic activity of the parasympathetic nervous system (67) in humans. Fixation frequencies to the whole picture, as well as to the defined eye region, were obtained for each monkey for SAL, 0.5 mg of NAL, 1 mg of NAL, and 2 mg of NAL. Fixations to the face and eye regions were normalized for each of the three

conditions by the SAL baseline for each animal. These normalized values were compared for fixations to the face and then for fixation to the eyes using ANOVA (with dose and image category as factors) and subsequent multiple comparison tests (Tukey–Kramer post hoc tests).

Data visualization using heat maps. Fixation coordinates to the faces of conspecific monkeys were determined using the correction procedure described previously (32). Heat maps were then plotted for each session based on fixations specifically to the face of the conspecific using the EyeMMV toolbox in MATLAB. Heat maps were based on the average number of fixations, measuring values within the SAL, NAL, OT, and OTNAL conditions to values ranging from less than 25 to greater than 250 fixations. Image dimensions were defined as 340 × 340 arbitrary units to align to the fixation data and binned at 20-unit intervals. Smoothing was accomplished using a Gaussian filter function in MATLAB. Fixations to the face of the conspecific were then averaged for all monkeys in a given condition and overlaid on a representative image of the face of one particular monkey. Difference heat maps were produced by comparing OTNAL over the SAL baseline (binned from less than −30 to greater than 60 fixation difference) as well as OTNAL over the added effects of the separate OT and NAL conditions (binned from less than −15 to greater than 30 fixation difference).

SI Results

NAL Dose–Response Curve. When the three doses of NAL were investigated for fixations to faces, an inverted U-shaped curve was observed, such that maximal effects clearly occurred following the 1-mg dose [Fig. S2*A*; $F(2,552) = 19.2$, $P < 0.001$ for main effect of doses, $P < 0.001$ for 1 mg over 2 mg, $P < 0.001$ for 1 mg over 0.5 mg, $P = 0.651$ for 0.5 mg over 2 mg, ANOVA with Tukey–Kramer post hoc tests]. When we examined fixations to the eyes, we found that monkeys overall preferred to look at conspecific eyes compared with human eyes [Fig. S2*B*; $F(1,546) = 8.9$, $P = 0.003$ for main effect of images], and the maximal effect again clearly occurred following the 1-mg dose [Fig. S2*B*; $F(2,546) = 13.6$, $P < 0.001$ for main effect of doses, $P < 0.001$ for 1 mg over 2 mg, $P < 0.001$ for 1 mg over 0.5 mg, $P = 0.762$ for 0.5 mg over 2 mg, ANOVA with Tukey–Kramer post hoc tests]. NAL administered nasally at the 1-mg dose was used subsequently for the remainder of the study.

Drug Effects on Fixation Duration Across All of the Behavioral Sessions. Although we noted a robust increase in the number of fixations to the face and eyes in the OTNAL condition across all of the behavioral sessions, it is also important to examine and confirm whether this increase in the number fixations may have been associated with a concurrent decrease in the duration of each individual fixation. To address this concern, we calculated the average duration of individual fixations for each individual pair of monkeys and compared the effects of drug conditions normalized to the SAL condition. For both the face and the eyes, we found no significant modulation of fixation duration for any drug condition relative to SAL [Fig. S3*A*, face: $F(3,76) = 1.1$, $P = 0.364$ for main effect, all $P > 0.410$ for individual comparisons; Fig. S3*B*, eyes: $F(3,76) = 0.84$, $P = 0.474$ for main effect, all $P > 0.399$ for individual comparisons, one-way ANOVA with Tukey–Kramer post hoc tests]. Thus, the effects of drug condition observed across all of the behavioral sessions appeared to be solely driven by modulations in the number of fixations.

Sex Differences. The number of macaques used in this study (three males and two females) is underpowered to explore potential sex differences fully. However, we separated monkeys based on sex and reanalyzed the data with both drug effect and the sex of the subject included as factors of interest for all of our positive results, including the increase in gaze to the face and eyes across all of the behavioral sessions, as well as increased attention to the conspecific following mutual eye contact and mutual reward. When analyzing the number of fixations to the face and eyes of a conspecific across all of the behavioral sessions, no significant effect of sex was found between animals within the SAL condition [face: 46.4 ± 8.1 fixations for males, 36.4 ± 10.1 fixations for females, $t(18) = 0.78$, $P = 0.447$; eyes: 17.4 ± 4.3 fixations for males, 9.5 ± 3.2 fixations for females, $t(18) = 1.35$, $P = 0.193$, two-sample t test]. We noted a significant main effect of drug condition but no significant main effect of sex or an interaction between these two factors [Fig. S6 *A* and *B*; face: main effect of drug $F(3,72) = 5.6$, $P = 0.002$; main effect of sex $F(1,72) = 0.17$, $P = 0.679$; interaction between drug and sex $F(3,72) = 0.91$, $P = 0.442$; eyes: main effect of drug $F(3,72) = 5.3$, $P = 0.002$; main effect of sex $F(1,72) = 1.03$, $P = 0.314$; interaction between drug and sex $F(3,72) = 0.62$, $P = 0.603$, two-way ANOVA with drug condition and sex as factors]. When analyzing gaze to the conspecific following mutual eye contact and mutual reward, again, no significant effect of sex was found between animals within the SAL condition [mutual eye contact: 0.097 ± 0.030 proportion of looking for males, 0.036 ± 0.015 proportion of looking for females, $t(18) = 1.19$, $P = 0.249$; mutual reward: 0.445 ± 0.081 proportion of looking for males, 0.506 ± 0.056 proportion of looking for females, $t(18) = 0.41$, $P = 0.686$, two-sample t test] (also no differences in baseline gaze dynamics between males and females with a larger sample size as reported in ref. 32). We noted a significant main effect of drug condition, but no significant main effect of sex or an interaction between these two factors [Fig. S6 *C* and *D*; mutual eye contact: main effect of drug $F(2,54) = 11.2$, $P < 0.0001$; main effect of sex $F(1,54) = 0.82$, $P = 0.368$; interaction between drug and sex $F(2,54) = 0.0004$, $P = 0.989$; mutual reward: main effect of drug $F(2,54) = 11.9$, $P < 0.0001$; main effect of sex $F(1,54) = 0.005$, $P = 0.816$; interaction between drug and sex $F(2,54) = 0.006$, $P = 0.942$, two-way ANOVA with drug condition and sex as factors]. Together, these results show that within our limited sample size, drug effects are observed indistinguishably across both sexes.

SI Discussion

With respect to OT and NAL administered alone, there are several studies to document the safety of applying these agents for therapeutic means. MacDonald et al. (68) conducted a systematic review of 38 randomized, controlled trials conducted between 1990 and 2010 investigating the safety, side effects, and subjective reactions to intranasal OT in humans. These authors reported that intranasal OT produces no detectable subjective changes in recipients and no reliable side effects, and that it is not associated with adverse outcomes when delivered in doses of 18–40 IU for short-term use in controlled research settings. NAL and naltrexone are potent, safe, and long-lasting opioid antagonists with minimal side effects. For example, naltrexone, although less selective to the μ-opioid receptor than NAL, has been used successfully to decrease self-injurious behavior, stereotypies, hyperactivity, and withdrawal while increasing verbal production and attentiveness (69, 70).

With regard to pharmacological administration, both OT and NAL are approved by the US Food and Drug Administration for intranasal delivery at our doses and are considered to have a low risk of side effects, which generally involve dizziness, flushing, weakness, nausea, and body aches. This route of administration has been validated for both OT (6, 71) and NAL (72–74) in previous human studies and could serve to minimize potential participant discomfort. OT has been used safely with chronic administration in recent clinical trials (5), and NAL has also been used safely with chronic administration in marketed therapies for opioid dependence (Suboxone; Reckitt Benckiser)

(intranasal NAL at a dose at least twofold higher than the dose used in the current study is a highly common and preferred method for reversing opioid overdose). Kerr et al. (62) compared the safety and effectiveness of NAL (2 mg/mL) given via the intranasal versus i.m. route in a randomized, controlled trial. A total of 172 patients suspected of heroin overdose were treated by emergency medical personnel and enrolled into the study: 83 patients received 1 mg per 0.5 mL into each nostril (2 mg total), and 89 patients received 2 mg/mL via the i.m. route. The adverse events seen were similar between the two groups; they were generally mild in nature and included agitation, nausea, and vomiting. Based on qualitative observations by several laboratory staff members, we observed no noticeable side effects of intranasal OTNAL, OT, or NAL in both laboratory and colony settings. However, more quantitative measurements (e.g., heart rate, blood pressure) should be measured in the future to document the safety of these administrations carefully.

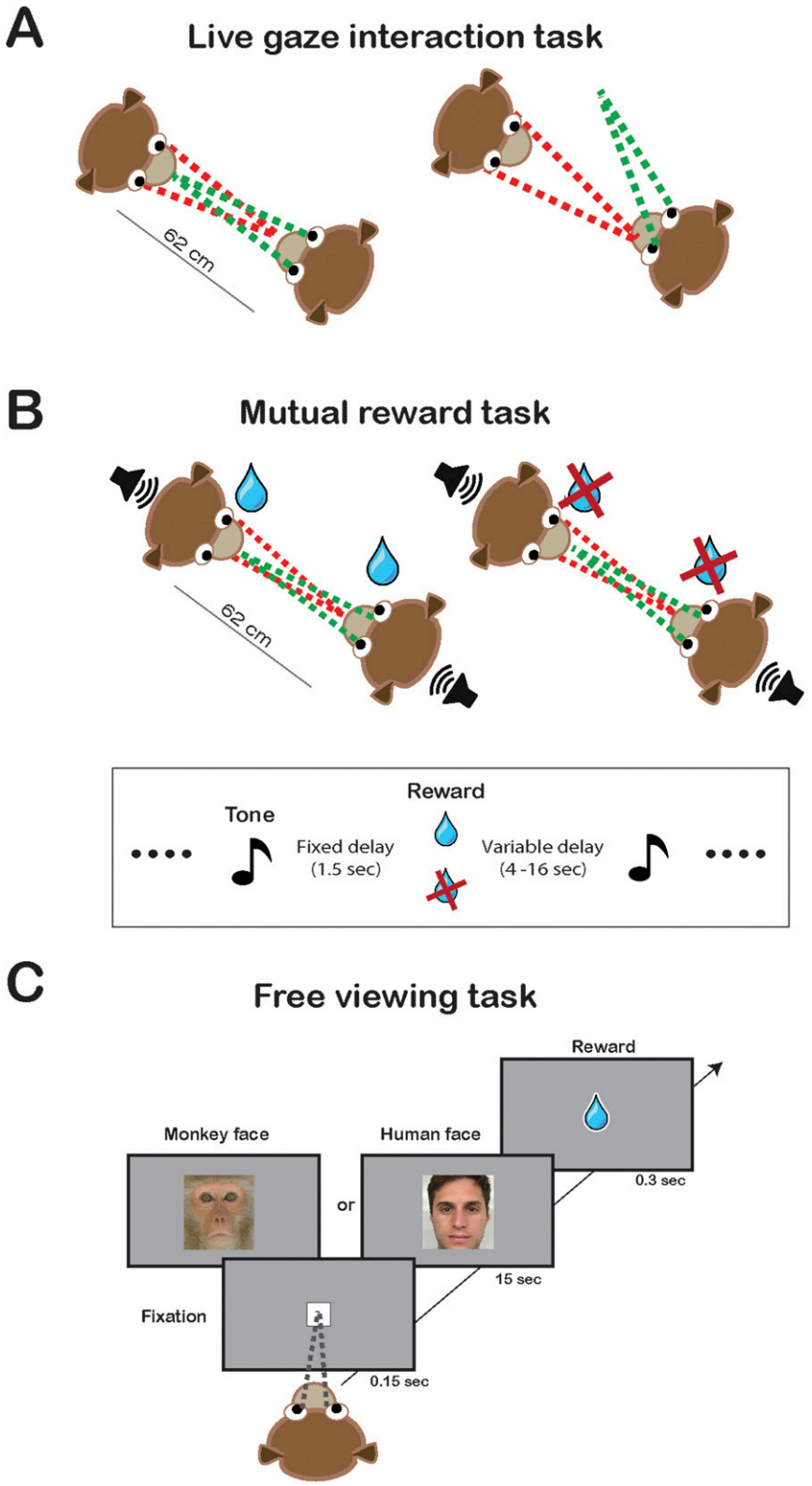

Fig. S1. Experimental designs. (*A*) Illustration of the live gaze interaction task used for examining social attention and its dynamics following mutual eye contact. The gaze positions of both monkeys in a given pair were recorded simultaneously and continuously. (*B*) Illustration of the mutual reward task used to examine the impact of context in social attention dynamics. This task setup was identical to the live gaze interaction task but included a tone that predicted mutual juice rewards or no juice rewards to both monkeys at equal probabilities after 1.5 s. The intertone interval between the tones was jittered from 4 to 16 s. (*C*) Illustration of the free-viewing task used to obtain an intranasal NAL dose–response curve. After fixating their gaze at the central target, monkeys viewed images for 15 s, followed by a reward in the form of a drop of juice.

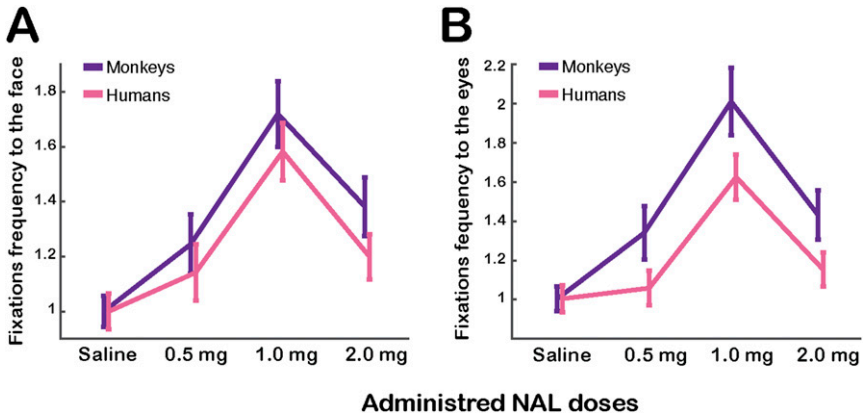

Fig. S2. NAL dose–response curve. (*A*) Overall frequency of fixations to the faces of conspecifics (purple) and to humans (pink, heterospecifics with similar facial features) after intranasally administering 0.5 mg, 1 mg, and 2 mg of NAL, normalized by the SAL condition. (*B*) Frequency of fixations to the eyes.

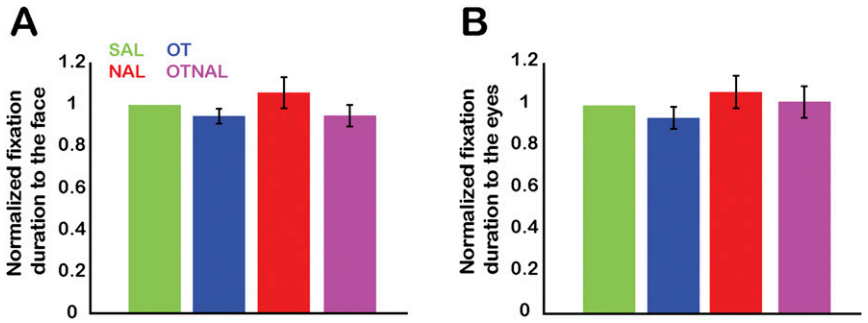

Fig. S3. Drug effects on fixation duration. (*A*) Overall fixation duration to the face of a conspecific in the OT (blue), NAL (red), and OTNAL (purple) conditions, normalized by the SAL (green) condition. (*B*) Overall fixation duration to the eyes of a conspecific in the same format as in *A*.

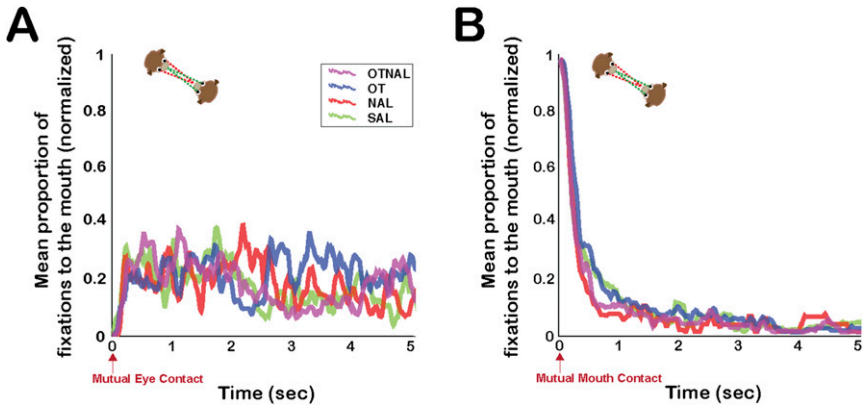

Fig. S4. Attention to the mouth following mutually interactive events in the live gaze interaction task is not modulated by drug condition. Peristimulus time histograms (PSTHs) show the proportions of looking at the mouth following mutual eye contact (*A*) and looking at the mouth following mutual gaze to the mouth of the conspecific (*B*) in the SAL (green), OT (blue), NAL (red), and OTNAL (purple) conditions. No 10-ms time bin for any drug condition was significantly higher than for SAL (all $P > 0.05$, paired-sample t tests).

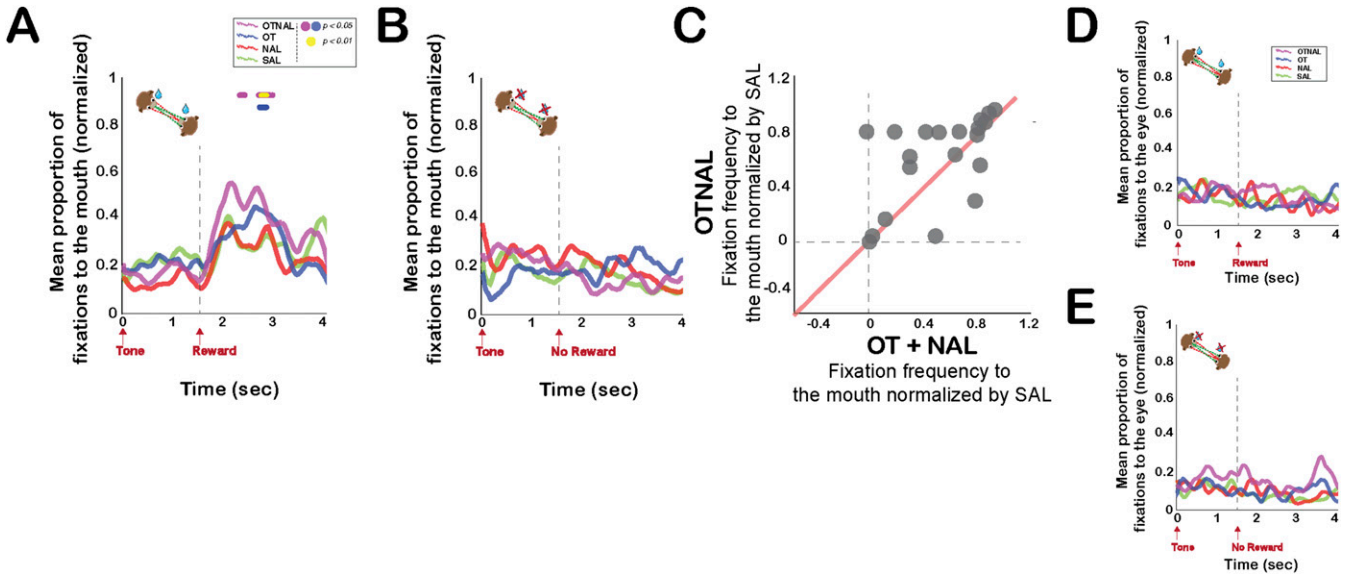

Fig. S5. Gaze dynamics following mutual reward receipt are driven by the mouth region of the conspecific. (*A*) PSTH shows the proportion of looking at the mouth following the tone predicting mutual reward receipt in the SAL (green), OT (blue), NAL (red), and OTNAL (purple) conditions. Reward occurred simultaneously for both monkeys 1.5 s after the tone. Horizontal marks indicate 10-ms time bins with significant differences ($P < 0.05$, OT over SAL, blue; $P < 0.05$, OTNAL over SAL, purple; $P < 0.01$, yellow; paired-sample *t* tests). (*B*) PSTH shows the proportion of looking at the mouth aligned to tones that did not result in reward to either monkey (same format as in *A*). No 10-ms time bin for any drug condition was significantly higher than for SAL (all $P > 0.05$, paired-sample *t* tests). (*C*) Effects size of OTNAL versus the summed effect size of OT and NAL alone for 1.5–3.5 s after mutual eye contact. (*D* and *E*) Same format as in *A* and *B*. A PSTH shows the proportion of looking at the eyes following a tone predicting mutual reward (*D*), and a PSTH shows the proportion of looking at the eyes aligned to tones that did not result in reward to either monkey (*E*). No 10-ms time bin for any drug condition was significantly higher than for SAL (all $P > 0.05$, paired-sample *t* tests).

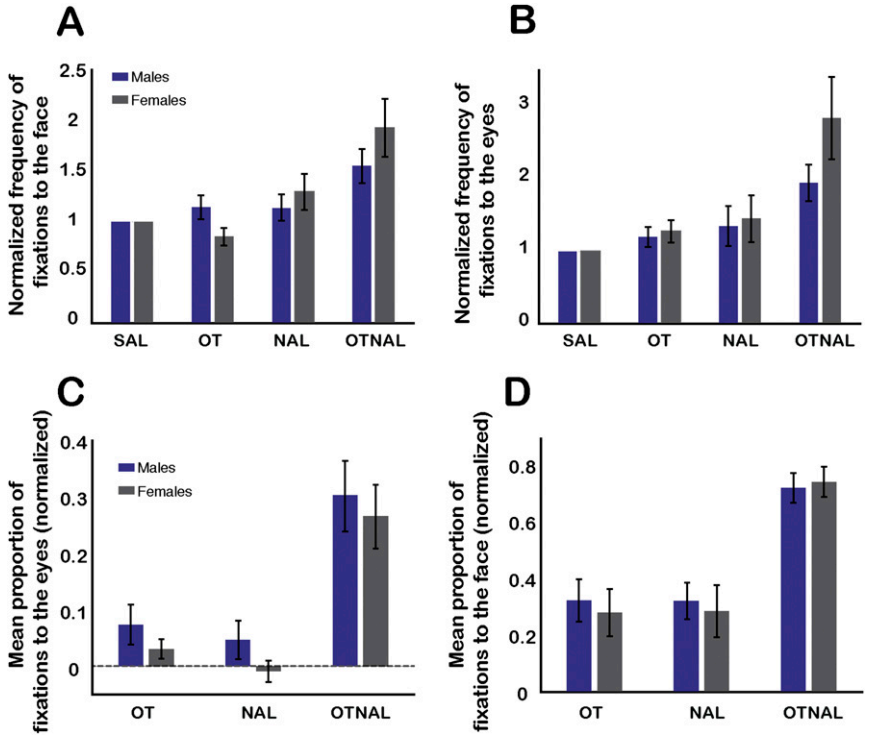

Fig. S6. Sex differences. (*A*) Overall frequency of gaze fixations to the face of a conspecific in the OT, NAL, and OTNAL conditions, normalized by the SAL condition for males (blue) and females (gray). (*B*) Overall frequency of gaze fixations to the eyes of a conspecific in the same format as in *A*. (*C*) Proportion of looking at the eyes following mutual eye contact in the OT, NAL, and OTNAL conditions, normalized by the SAL condition for males (blue) and females (gray). (*D*) Proportion of looking at the face following mutual reward in the same format as in *C*.

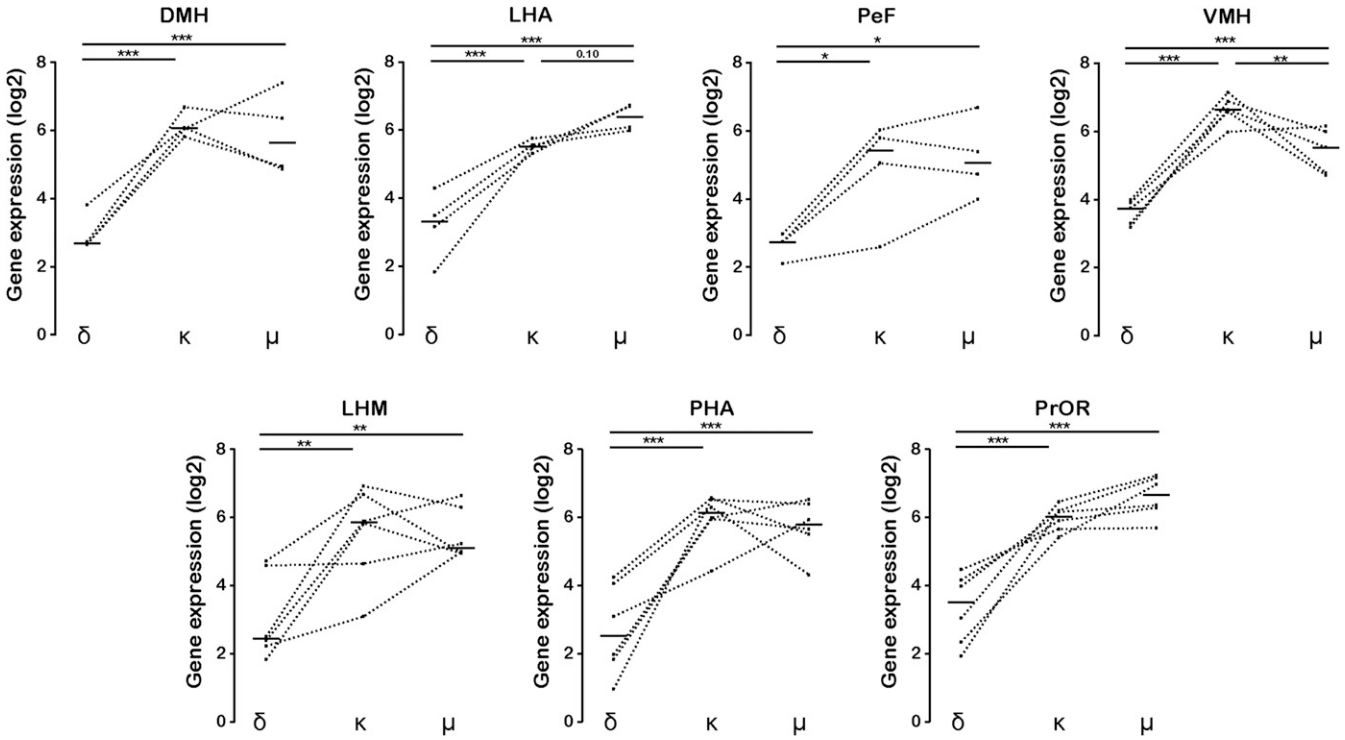

Fig. S7. μ-Opioid and κ-opioid receptors display significantly greater expression than δ-opioid receptors in *OXT*-enriched regions. Shown are the seven *OXT*-enriched regions of 10 that are not shown in Fig. 4*B*. Each line connects samples from the same donor. Different numbers of lines are due to nonuniform sampling across the six Allen Human Brain Atlas donors. The horizontal ticks indicate the mean of different donors. Dorsomedial hypothalamic nucleus (DMH): $F(1,3) = 13.25$, $P = 0.036$ for main effect, $P < 0.001$ for μ over δ, $P < 0.001$ for κ over δ, $P = 0.654$ for μ over κ; one-way within-subjects ANOVA with Benjamini–Hochberg-corrected post hoc tests; lateral hypothalamic area (LHA) $F(1,3) = 22.68$, $P = 0.018$ for main effect, $P < 0.001$ for μ over δ, $P < 0.001$ for κ over δ, $P = 0.096$ for μ over κ; perifornical nucleus (PeF): $F(1,3) = 36.82$, $P = 0.009$ for main effect, $P = 0.034$ for μ over δ, $P = 0.034$ for κ over δ, $P = 0.691$ for μ over κ; ventral hypothalamic area (VMH) $F(1,4) = 18.30$, $P = 0.013$ for main effect, $P < 0.001$ for μ over δ, $P < 0.001$ for κ over δ, $P = 0.003$ for κ over μ; lateral hypothalamic area (LHM): $F(1,5) = 13.26$, $P = 0.015$ for main effect, $P = 0.004$ for μ over δ, $P = 0.004$ for κ over δ, $P = 0.999$ for μ over κ; posterior hypothalamic area (PHA): $F(1,5) = 14.05$, $P = 0.013$ for main effect, $P < 0.001$ for μ over δ, $P < 0.001$ for κ over δ, $P = 0.686$ for μ over κ; preoptic region (PrOR): $F(1,5) = 25.32$, $P = 0.004$ for main effect, $P < 0.001$ for μ over δ, $P < 0.001$ for κ over δ, $P = 0.141$ for μ over κ. $^*P < 0.05$, $^{**}P < 0.01$, $^{***}P < 0.001$.

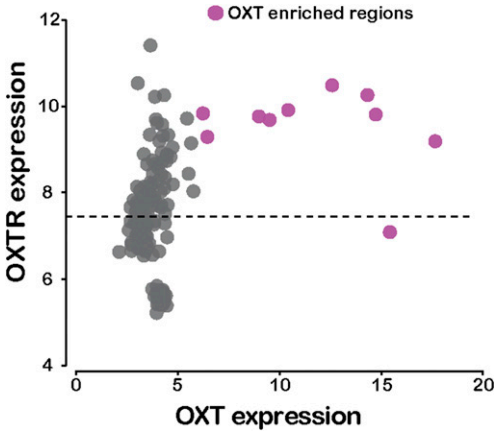

Fig. S8. *OXTR* expression is consistently above average within *OXT*-enriched regions (same format as in Fig. 4*C*).

Table S1. One hundred ninety regions analyzed that contained samples from at least four of six Allen Human Brain Atlas donors

Structure category	Structure name	Acronym	HEX
Frontal lobe	Zona incerta	ZI	FF5D62
Frontal lobe	Ventral tegmental area	VTA	FF5D62
Frontal lobe	Inferior frontal gyrus, triangular part	trIFG	FF5D62
Frontal lobe	Transverse gyri	TG	FF5D62
Frontal lobe	Tail of the caudate nucleus	TCd	FF5D62
Frontal lobe	Superior temporal gyrus, lateral bank of gyrus	STG-l	FF5D62
Frontal lobe	Superior temporal gyrus, inferior bank of gyrus	STG-i	FF5D62
Frontal lobe	Superior parietal lobule, superior bank of gyrus	SPL-s	FF5D62
Frontal lobe	Superior parietal lobule, inferior bank of gyrus	SPL-i	FF5D62
Frontal lobe	Spinal trigeminal nucleus	Sp5	FF5D62
Frontal lobe	Superior occipital gyrus, superior bank of gyrus	SOG-s	FF5D62
Frontal lobe	Substantia nigra, pars reticulata	SNR	FF5D62
Frontal lobe	Substantia nigra, pars compacta	SNC	FF5D62
Frontal lobe	Supramarginal gyrus, superior bank of gyrus	SMG-s	FF5D62
Frontal lobe	Supramarginal gyrus, inferior bank of gyrus	SMG-i	FF5D62
Frontal lobe	Short insular gyri	SIG	FF5D62
Frontal lobe	Superior frontal gyrus, medial bank of gyrus	SFG-m	FF5D62
Frontal lobe	Superior frontal gyrus, lateral bank of gyrus	SFG-l	FF5D62
Frontal lobe	Subthalamic nucleus	Sb	FF5D62
Frontal lobe	Subiculum	S	FF5D62
Frontal lobe	Red nucleus	RN	FF5D62
Frontal lobe	Raphe nuclei of medulla	RaM	FF5D62
Parietal lobe	Reticular nucleus of thalamus	R	E9BF59
Parietal lobe	VIIB, paravermis	PV-VIIB	E9BF59
Parietal lobe	VI, paravermis	PV-VI	E9BF59
Parietal lobe	V, paravermis	PV-V	E9BF59
Parietal lobe	IV, paravermis	PV-IV	E9BF59
Parietal lobe	Crus II, paravermis	PV-Crus II	E9BF59
Parietal lobe	Crus I, paravermis	PV-Crus I	E9BF59
Parietal lobe	Putamen	Pu	E9BF59
Parietal lobe	Preoptic region	PrOR	E9BF59
Parietal lobe	Precentral gyrus, superior lateral aspect of gyrus	PrG-sl	E9BF59
Parietal lobe	Precentral gyrus, bank of the precentral sulcus	PrG-prc	E9BF59
Parietal lobe	Precentral gyrus, inferior lateral aspect of gyrus	PrG-il	E9BF59
Temporal lobe	Pontine reticular formation	PRF	FF9200
Temporal lobe	Postcentral gyrus, superior lateral aspect of gyrus	PoG-sl	FF9200
Temporal lobe	Postcentral gyrus, bank of the central sulcus	PoG-cs	FF9200
Temporal lobe	Pontine nuclei	Pn	FF9200
Temporal lobe	Planum polare	PLP	FF9200
Temporal lobe	Parahippocampal gyrus, lateral bank of gyrus	PHG-l	FF9200
Temporal lobe	Parahippocampal gyrus, bank of the cos	PHG-cos	FF9200
Temporal lobe	Posterior hypothalamic area	PHA	FF9200
Temporal lobe	Precuneus, superior lateral bank of gyrus	Pcu-s	FF9200
Temporal lobe	Precuneus, inferior lateral bank of gyrus	Pcu-i	FF9200
Temporal lobe	Paracentral lobule, anterior part, inferior bank of gyrus	PCLa-i	FF9200
Temporal lobe	Occipitotemporal gyrus, superior bank of gyrus	OTG-s	FF9200
Temporal lobe	Occipitotemporal gyrus, inferior bank of gyrus	OTG-i	FF9200
Temporal lobe	Inferior frontal gyrus, orbital part	orIFG	FF9200
Temporal lobe	Middle temporal gyrus, superior bank of gyrus	MTG-s	FF9200
Temporal lobe	Middle temporal gyrus, inferior bank of gyrus	MTG-i	FF9200
Temporal lobe	Medial orbital gyrus	MOrG	FF9200
Occipital lobe	Medial geniculate complex	MG	E87651
Occipital lobe	Middle frontal gyrus, superior bank of gyrus	MFG-s	E87651
Occipital lobe	Middle frontal gyrus, inferior bank of gyrus	MFG-i	E87651
Occipital lobe	Lateral orbital gyrus	LOrG	E87651
Occipital lobe	Lateral medullary reticular group	LMRt	E87651
Occipital lobe	Lingual gyrus, striate	LiG-str	E87651
Occipital lobe	Lingual gyrus, peristriate	LiG-pest	E87651
Occipital lobe	Long insular gyri	LIG	E87651
Occipital lobe	Lateral hypothalamic area, mammillary region	LHM	E87651
Occipital lobe	Dorsal lateral geniculate nucleus	LGd	E87651
Insula	Lateral nucleus	LA	FFF162

Table S1. Cont.

Structure category	Structure name	Acronym	HEX
Insula	Inferior temporal gyrus, bank of mts	ITG-mts	FFF162
Cingulate	Inferior temporal gyrus, lateral bank of gyrus	ITG-l	7E5B33
Cingulate	Inferior temporal gyrus, bank of the its	ITG-its	7E5B33
Cingulate	Inferior olivary complex	IO	7E5B33
Cingulate	Rostral group of intralaminar nuclei	ILr	7E5B33
Cingulate	Caudal group of intralaminar nuclei	ILc	7E5B33
Cingulate	Heschl's gyrus	HG	7E5B33
Hippocampus	VIIIA, lateral hemisphere	He-VIIIA	FEBA65
Hippocampus	VIIB, lateral hemisphere	He-VIIB	FEBA65
Hippocampus	VI, lateral hemisphere	He-VI	FEBA65
Hippocampus	Crus II, lateral hemisphere	He-Crus II	FEBA65
Hippocampus	Crus I, lateral hemisphere	He-Crus I	FEBA65
Hippocampus	Head of the caudate nucleus	HCd	FEBA65
Parahippocampus	Gyrus rectus	GRe	B48D3F
Parahippocampus	Globus pallidus, internal segment	GPi	B48D3F
Amygdala	Gigantocellular group	GiRt	00B4AA
Amygdala	Fusiform gyrus, bank of the its	FuG-its	00B4AA
Amygdala	Fusiform gyrus, bank of cos	FuG-cos	00B4AA
Amygdala	Frontal operculum	fro	00B4AA
Amygdala	Posterior group of nuclei	DTP	00B4AA
Amygdala	Medial group of nuclei	DTM	00B4AA
Basal ganglia	Lateral group of nuclei, ventral division	DTLv	4BE7B8
Basal ganglia	Lateral group of nuclei, dorsal division	DTLd	4BE7B8
Basal ganglia	Anterior group of nuclei	DTA	4BE7B8
Basal ganglia	Dentate nucleus	Dt	4BE7B8
Basal ganglia	Dentate gyrus	DG	4BE7B8
Basal ganglia	Cuneus, striate	Cun-str	4BE7B8
Basal ganglia	Cuneus, peristriate	Cun-pest	4BE7B8
Basal forebrain	Cuneate nucleus	Cu	5A7DFE
Basal forebrain	Corticomedial group	COMA	5A7DFE
Basal forebrain	Claustrum	Cl	5A7DFE
Basal forebrain	Cingulate gyrus, parietal part, superior bank of gyrus	CgGp-s	5A7DFE
Basal forebrain	Cingulate gyrus, parietal part, inferior bank of gyrus	CgGp-i	5A7DFE
Basal forebrain	Cingulate gyrus, frontal part, superior bank of gyrus	CgGf-s	5A7DFE
Mammillary region	Cingulate gyrus, frontal part, inferior bank of gyrus	CgGf-i	FE61DE
Mammillary region	Central nucleus	CeA	FE61DE
Mammillary region	Corpus callosum	cc	FE61DE
Mammillary region	CA4 field	CA4	FE61DE
Mammillary region	CA3 field	CA3	FE61DE
Mammillary region	CA2 field	CA2	FE61DE
Anterior hypothalamic region	CA1 field	CA1	895AFE
Anterior hypothalamic region	Basomedial nucleus	BMA	895AFE
Anterior hypothalamic region	Basolateral nucleus	BLA	895AFE
Hypothamalus_tuberal	Body of the caudate nucleus	BCd	00ACEA
Hypothamalus_tuberal	Amygdalohippocampal transition zone	ATZ	00ACEA
Hypothamalus_tuberal	Arcuate nucleus of medulla	Arc	00ACEA
Hypothamalus_tuberal	Angular gyrus, superior bank of gyrus	AnG-s	00ACEA
Hypothamalus_tuberal	Angular gyrus, inferior bank of gyrus	AnG-i	00ACEA
Preoptic region	Nucleus accumbens	Acb	003BEB
Subthalamus	Vestibular nuclei	8Ve	00E879
Thalamus	Ventromedial hypothalamic nucleus	VMH	00D132
Thalamus	Temporal pole, superior aspect	TP-s	00D132
Thalamus	Temporal pole, medial aspect	TP-m	00D132
Thalamus	Subcuneiform nucleus	SubCn	00D132
Thalamus	Nucleus subceruleus	SubC	00D132
Thalamus	Superior rostral gyrus	SRoG	00D132
Thalamus	Septal nuclei	SptN	00D132
Thalamus	Superior occipital gyrus, inferior bank of gyrus	SOG-i	00D132
Thalamus	Superior olivary complex	SOC	00D132
Thalamus	Supraoptic nucleus	SO	00D132
Thalamus	Subcallosal cingulate gyrus	SCG	00D132
Cerebellum	Pontine raphe nucleus	RPn	A9EBED

Table S1. Cont.

Structure category	Structure name	Acronym	HEX
Cerebellum	Paraventricular nucleus of the hypothalamus	PVH	A9EBED
Cerebellum	VIIIB, paravermis	PV-VIIIB	A9EBED
Cerebellum	VIIIA, paravermis	PV-VIIIA	A9EBED
Cerebellum	IX, paravermis	PV-IX	A9EBED
Cerebellum	Precentral gyrus, bank of the central sulcus	PrG-cs	A9EBED
Cerebellum	Posterior orbital gyrus	POrG	A9EBED
Cerebellum	Postcentral gyrus, bank of the posterior central sulcus	PoG-pcs	A9EBED
Cerebellum	Postcentral gyrus, inferior lateral aspect of gyrus	PoG-il	A9EBED
Cerebellum	Paracentral lobule, anterior part, superior bank of gyrus	PCLa-s	A9EBED
Cerebellum	Parolfactory gyri	PaOG	A9EBED
Cerebellum	Medial parabrachial nucleus	MPB	A9EBED
Cerebellum	Motor nucleus of trigeminal nerve	Mo5	A9EBED
Cerebellum	Midbrain raphe nuclei	MBRa	A9EBED
Cerebellum	Lateral parabrachial nucleus	LPB	A9EBED
Cerebellum	Inferior rostral gyrus	IRoG	A9EBED
Cerebellum	Inferior occipital gyrus, superior bank of gyrus	IOG-s	A9EBED
Cerebellum	Inferior occipital gyrus, inferior bank of gyrus	IOG-i	A9EBED
Cerebellum	Globus pallidus, external segment	GPe	A9EBED
Cerebellum	Fusiform gyrus, lateral bank of gyrus	FuG-l	A9EBED
Cerebellum	Central gray substance of midbrain	CGMB	A9EBED
Cerebellum	Cochlear nuclei	8Co	A9EBED
Cerebellum	Facial motor nucleus	7	A9EBED
Cerebellum	Abducens nucleus	6	A9EBED
Cerebellum	VIIIB	Ve-VIIIB	A9EBED
Cerebellum	VIIIA	Ve-VIIIA	A9EBED
Cerebellum	VIIB	Ve-VIIB	A9EBED
Cerebellum	VIIAt	Ve-VIIAt	A9EBED
Cerebellum	VI	Ve-VI	A9EBED
Pons	V	Ve-V	8ED6C4
Pons	IX	Ve-IX	8ED6C4
Pons	IV	Ve-IV	8ED6C4
Pons	III	Ve-III	8ED6C4
Pons	Temporal pole, inferior aspect	TP-i	8ED6C4
Pons	Tuberomammillary nucleus	TM	8ED6C4
Pons	Supramammillary nucleus	SuM	8ED6C4
Pons	Superior colliculus	SC	8ED6C4
Pons	III, paravermis	PV-III	8ED6C4
Pons	Principal sensory nucleus of trigeminal nerve	Pr5	8ED6C4
Pons	Planum temporale	PLT	8ED6C4
Pons	Perifornical nucleus	PeF	8ED6C4
Midbrain tectum	Inferior frontal gyrus, opercular part	opIFG	64A494
Midbrain tectum	Olfactory tubercle	OlfT	64A494
Midbrain tegmentum	Basal nucleus of Meynert	nbM	6C93A3
Midbrain tegmentum	Medial mammillary nucleus	MM	6C93A3
Midbrain tegmentum	Lateral tuberal nucleus	LTu	6C93A3
Midbrain tegmentum	Lateral mammillary nucleus	LM	6C93A3
midbrain tegmentum	Lateral hypothalamic area, tuberal region	LHT	6C93A3
Midbrain tegmentum	Lateral hypothalamic area, anterior region	LHA	6C93A3
Midbrain tegmentum	Locus ceruleus	LC	6C93A3
Midbrain tegmentum	Inferior colliculus	IC	6C93A3
Midbrain tegmentum	VIIIB, lateral hemisphere	He-VIIIB	6C93A3
Claustrum	V, lateral hemisphere	He-V	6570A4
Myelencephalon	IV, lateral hemisphere	He-IV	9F54A6
Myelencephalon	Globose nucleus	Glo	9F54A6
Myelencephalon	Dorsomedial hypothalamic nucleus	DMH	9F54A6
Myelencephalon	Nucleus of the diagonal band, horizontal division	DBv	9F54A6
Myelencephalon	Nucleus of the diagonal band, vertical division	DBh	9F54A6
Myelencephalon	Cuneiform nucleus	CnF	9F54A6
Myelencephalon	Central medullary reticular group	CMRt	9F54A6
Myelencephalon	Central glial substance	CGS	9F54A6
Myelencephalon	Cingulate gyrus, retrosplenial part, superior bank of gyrus	CgGr-s	9F54A6
Myelencephalon	Bed nucleus of stria terminalis	BST	9F54A6

Table S1. Cont.

Structure category	Structure name	Acronym	HEX
Myelencephalon	Anterior orbital gyrus	AOrG	9F54A6
Myelencephalon	Oculomotor nuclear complex	3	9F54A6
Myelencephalon	Hypoglossal nucleus	12	9F54A6
White matter	Dorsal motor nucleus of the vagus	10	827E79

"Structure category" refers to the anatomical ontological category of each tissue sample, which was derived from annotations in the Allen Institute data and is displayed in Fig. 4*A*. "Structure name" and "Structure acronym" refer to the anatomical name and abbreviation of each tissue sample as it appears in the Allen Institute data. "HEX" provides the hexadecimal color code of each structure category as it appears in Fig. 4*A*. cos, collateral sulcus; its, inferior temporal sulcus; mts, middle temporal sulcus.